


Synthesis, characterization and antimicrobial activity of zinc(II) ibuprofen complexes with nitrogen-based ligands

Hijazi Abu Ali, Suhad N. Omar, Mohanad D. Darawsheh & Hadeel Fares


To cite this article: Hijazi Abu Ali, Suhad N. Omar, Mohanad D. Darawsheh & Hadeel Fares (2016) Synthesis, characterization and antimicrobial activity of zinc(II) ibuprofen complexes with nitrogen-based ligands, Journal of Coordination Chemistry, 69:6, 1110-1122, DOI: [10.1080/00958972.2016.1149819](https://doi.org/10.1080/00958972.2016.1149819)

To link to this article: <https://doi.org/10.1080/00958972.2016.1149819>

 View supplementary material [↗](#)


 Published online: 01 Mar 2016.

 Submit your article to this journal [↗](#)

 Article views: 646

 View related articles [↗](#)

 View Crossmark data [↗](#)

 Citing articles: 20 View citing articles [↗](#)

Synthesis, characterization and antimicrobial activity of zinc(II) ibuprofen complexes with nitrogen-based ligands

Hijazi Abu Ali[‡], Suhad N. Omar[‡], Mohanad D. Darawsheh and Hadeel Fares

Department of Chemistry, Birzeit University, Birzeit, Palestine

ABSTRACT

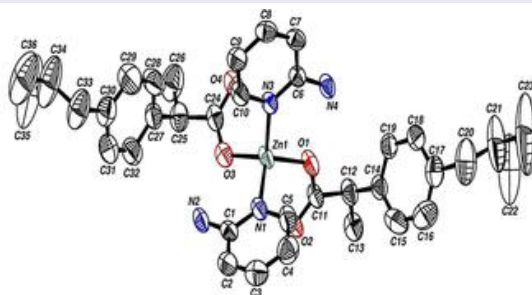
Metal carboxylate complexes possess different carboxylate coordination modes, e.g. monodentate, bidentate, and bridging bidentate. Five Zn(II) complexes were prepared and characterized in order to examine their coordination modes in addition to their biological activity. The syntheses were started by preparation of $[\text{Zn}(\text{ibup})_2(\text{H}_2\text{O})_2]$ (**1**). Then, different nitrogen-donor ligands reacted with **1** to produce $[\text{Zn}(\text{ibup})_2(2\text{-ampy})_2]$ (**2**), $[\text{Zn}(\text{ibup})(2\text{-ammethylpy})]$ (**3**), $[\text{Zn}(\text{ibup})(2,2'\text{-bipy})]$ (**4**), and $[\text{Zn}_2(\text{ibup})_4(2\text{-methylampy})_2]$ (**5**) (ibup = ibuprofen, 2-ampy = 2-aminopyridine, 2-ammethylpy = 2-aminomethylpyridine, 2,2'-bipy = 2,2'-bipyridine, 2-methylampy = 2-(methylamino)pyridine). IR, ^1H NMR, $^{13}\text{C}\{^1\text{H}\}$ -NMR and UV–vis spectroscopies were used for characterization. The crystal structures of **2** and **5** were determined by single-crystal X-ray diffraction. Investigation of *in vitro* antibacterial activities for the complexes against Gram-positive (*Micrococcus luteus*, *Staphylococcus aureus* and *Bacillus subtilis*) and Gram-negative (*Escherichia coli*, *Klebsiella pneumoniae* and *Proteus mirabilis*) bacteria were done using agar well-diffusion method. Complex **1** showed antibacterial activity against Gram-positive bacteria. Complexes **2** and **3** did not exhibit antibacterial activity. Complex **4** showed antibacterial activity and was chosen for further studies to determine the inhibition zone diameter for different concentrations and to set the minimum inhibitory concentration. The antibacterial activity against most of the bacteria was minimized as a result of the complexation of zinc ibuprofen with 2,2'-bipy in **4**.


ARTICLE HISTORY


Received 14 September 2015
Accepted 12 January 2016

KEYWORDS

Zinc(II) ibuprofen complexes;
nitrogen-donor ligands;
antibacterial activity;
inhibition zone diameter;
minimum inhibition
concentration



CONTACT Hijazi Abu Ali  habuali@birzeit.edu; habuali1@yahoo.com

 Supplemental data for this article can be accessed <http://dx.doi.org/10.1080/00958972.2016.1149819>

[‡]These authors contributed equally to this work.

1. Introduction

The average human body contains *ca.* 3 g of zinc, which makes it the second most abundant trace element in the body after iron [1–4]. Zinc is the only metal that appears in all enzyme classes [1, 4]. It is mainly distributed in the blood, kidney, liver and bone [5]. Studies have shown that Zn(II) has important antibacterial and antiviral effects [6], and high zinc ion concentrations may have some antibacterial properties [7]. In addition, zinc inhibits the growth of many bacteria, e.g., *Escherichia coli*, *Streptococcus faecalis* and some strains of soil bacteria [8].

Heterocyclic organic compounds enter the formulations of many vitamins and drugs, playing an important role in biological systems. The literature indicates that ligands/drugs become more bacteriostatic upon complexation with transition metals as compared to unchelated ones [9]. Antimicrobial activity of nonsteroidal anti-inflammatory drugs (NSAIDs) have been reported [9a]. The antimicrobial activity of these NSAIDs was enhanced when complexed with metals and other nitrogen-based ligands [9a]. Several metal complexes accelerate the drug action and the efficacy of the organic therapeutic agent; Co(II) complexes with the NSAID mefenamic acid as ligand have been investigated as potential anti-inflammatory agents [9b]. Several research groups also reported Cu(II) complexes of mefenamic acid, naproxen, diclofenac [9c], diflunisal [9d], and flufenamic acid [9e]. Co(II) complexes of naproxen [9f] and tolfenamic acid [9g] and Mn(II) complexes of tolfenamic acid [9h] have also shown anti-inflammatory activity. Zinc complexes with bioactive ligands have pharmaceutical effects because they can catalyze many enzymatic processes in biological systems; zinc(II) aliphatic carboxylates (like valproic acid) [10, 11] and aromatic carboxylates (like naproxen) [12] have been synthesized and studied as antibacterial and anti-malarial and in other biological fields [8, 13].

Ibuprofen “ibupH” (figure 1) is a NSAID. There are many side effects associated with the clinical use of NSAIDs. Therefore, numerous studies were performed to reduce these side effects. One successful strategy was the use of d-block metal complexes of NSAIDs as therapeutic agents. This approach is based on the observation that some d-block metal ions, such as Cu(II) and Zn(II), can act as anti-inflammatory agents [14, 15]; or sometimes this interaction may lead to a better understanding of the metal ion antagonism [16]. For example, the Zn(II) complex of aspirin has a better therapeutic index (2.64 times) than aspirin itself and has improved physicochemical characteristics. The Zn-aspirin complex is more effective in therapy and less ulcerogenic than either aspirin alone or a physical mixture of aspirin and ZnSO₄ [17–19].

The coordination of transition metals, and especially d¹⁰ metal ions such as Cd(II) and Zn(II), with the anti-inflammatory carboxylate agents tolmetin, ibuprofen, and naproxen was studied to examine their binding mode [12, 20–25]. Cu(II) ibuprofen with 2,2'-bipyridine (2,2-bipy), 1,10-phenanthroline (1,10-phen), and 2,9-dmphenan were synthesized and characterized [26]. The antimicrobial activity of the copper(II) complex of the fluoroquinolone antibacterial drug *N*-propyl-norfloxacin (Hpr-norf) in the presence of phenanthroline has been tested, revealing increased potency in comparison to free Hpr-norf (minimum inhibition concentration, MIC = 4–16 μg mL⁻¹) [27].

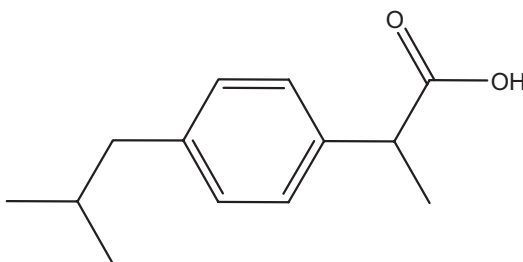


Figure 1. Structure of ibuprofen.

Typically, ibuprofen is produced industrially as a racemate. The compound contains a chiral center in the α -position of the propionate. Hence, it has two enantiomers, dextrorotatory (*S*), and the levorotatory (*R*). The biological effects and metabolism for the two enantiomers are different and the *S*-(+)-ibuprofen was found to be the active form [26].

Nitrogen-based ligand derivatives, carboxylate derivatives, and the Zn(II) cation are of interest due to their potential activity against different types of bacteria. Hence, we combine the three derivatives in one complex to enhance their biological activity. In the present work, the synthesis, characterization and antibacterial activity of new zinc(II) ibuprofen containing complexes with 2-aminopyridine (2-ampy), 2-aminomethylpyridine (2-ammethylpy), 2,2'-bipy and 2-(methylamino)pyridine (2-methylampy) are described. The crystal structures of $[\text{Zn}(\text{ibup})_2(2\text{-ampy})_2]$ (**2**) and $[\text{Zn}_2(\text{ibup})_4(2\text{-methylampy})_2]$ (**5**) are reported.

2. Results and discussion

2.1. Synthesis of zinc complexes

$[\text{Zn}(\text{ibup})_2(\text{H}_2\text{O})_2]$ (**1**) was prepared by mixing zinc chloride and sodium ibuprofen aqueous solutions in 1 : 2 M ratio. The desired product was obtained as a white solid (scheme 1), structure of **1** was previously determined [26]. Mixed-ligand zinc(II) complexes were prepared by adding the appropriate *N*-donor ligand to the water insoluble **1** (scheme 2). The physical properties of **1-5** are summarized in table S1.

2.2. Crystallographic study of 2

The atomic numbering scheme and atom connectivity for **2** are shown in figure 2. The asymmetric unit of **2** contains a Zn(II) cation, two ibuprofen ligands and two 2-ampy ligands.

Table 1. Selected bond lengths (Å) and angles (°) for **2**.

Bond distance (Å)		Bond angle (°)		Bond angle (°)	
N(1)–Zn(1)	2.055(3)	C(5)–N(1)–Zn(1)	114.6(3)	C(11)–O(1)–Zn(1)	119.1(2)
N(3)–Zn(1)	2.043(3)	C(1)–N(1)–Zn(1)	126.6(3)	O(3)–Zn(1)–O(1)	123.29(12)
O(1)–Zn(1)	1.920(2)	O(3)–Zn(1)–N(1)	105.06(13)	O(3)–Zn(1)–N(3)	110.49(12)
O(3)–Zn(1)	1.907(3)	O(1)–Zn(1)–N(1)	110.01(13)	O(1)–Zn(1)–N(3)	106.53(10)
		N(3)–Zn(1)–N(1)	98.75(11)		

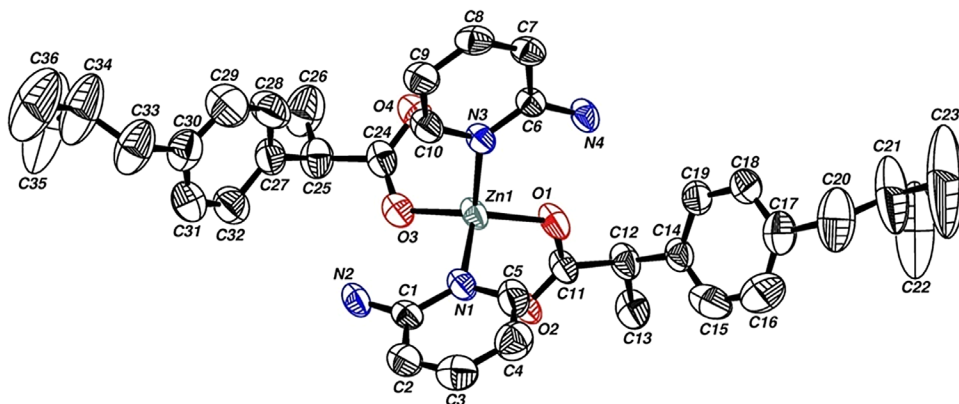
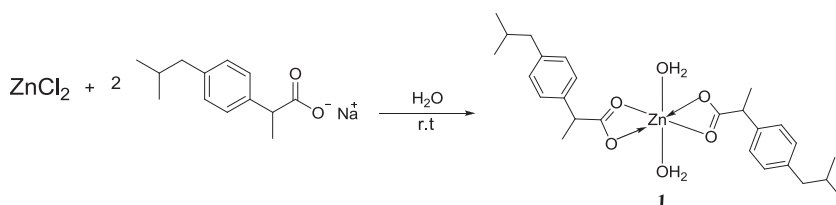
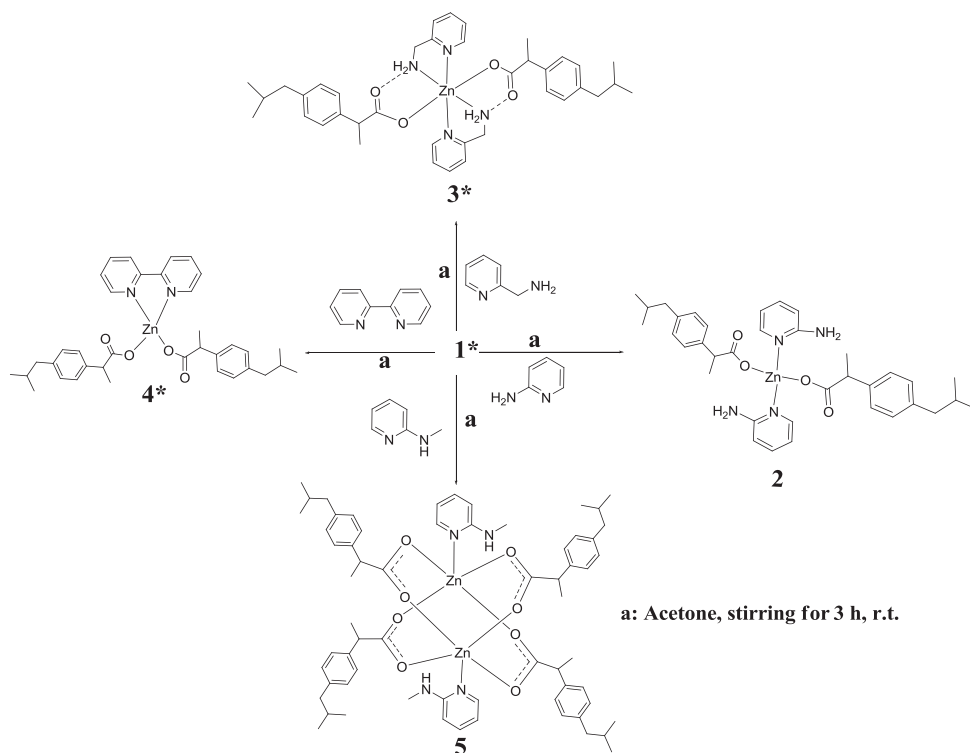


Figure 2. The molecular structure of **2** showing the atom labeling scheme.



Scheme 1. Synthesis of **1**.



Scheme 2. Synthesis and the proposed structures of **2–5** (*: proposed structure).

Zn(II) is surrounded by two monodentate ibuprofen ligands with O–Zn coordination distances of 1.920(2) Å and 1.907(3) Å, which are a little shorter than similar reported distances [28, 29]. The 2-ampy ligands with distances involving pyridyl nitrogen and Zn being 2.055(3) Å and 2.043(3) Å are similar to previously reported distances (2.048 Å in average) [28, 29]. Selected bond distances and angles are tabulated in table 1.

Zn(II) has a distorted tetrahedral geometry. The deviation from regular tetrahedral is observed from binding angles O3–Zn1–O1 = 123.29(12)°, O3–Zn1–N3 = 110.49(12)°, O1–Zn1–N3 = 106.53(10)°, O3–Zn1–N1 = 105.06(13)°, O1–Zn1–N1 = 110.01(13)° and N3–Zn1–N1 = 98.75(11)°. Intramolecular and intermolecular hydrogen bonds are shown in table S2. The first two bonds belong to the former while the last two bonds belong to the latter type.

The Zn–O distances for **2** are 1.84–2.33 Å, typical of monodentate acetate complexes [30]. The average C–O bond distance of coordinated oxygen is 1.273 Å, while the average of non-coordinated C–O oxygen is 1.212 Å. The difference in bond distances between the coordinated and non-coordinated C–O are considered an indication of non-delocalization of ibuprofen due to monodentate coordination. The average O–C–O bond angle in **2** is 123.8° as expected for monodentate carboxylate coordination [10–12].

2.3. Crystallographic study of **5**

The atom numbering scheme and connectivity for **5** are shown in figure 3. The structure consists of centrosymmetric binuclear Zn units, with four ibuprofen bridging bidentate carboxylate residues. Each Zn(II) has a square pyramidal coordination geometry with the apex provided by axial coordination of 2-methylampy. Selected bond distances and angles are tabulated in table 2.

The Zn(1)⋯Zn(1)#1 distance in **5** is 3.0073(7) Å and lies within the average distance for four-coordinate binuclear Zn clusters, [2.9–3.0 Å] [31]. The corresponding Zn⋯Zn distance observed in [Zn₂(valp)₄(quin)₂] is [2.9481(3) Å] [10]; thus, the Zn⋯Zn distance in **5** is large enough to conclude no direct Zn–Zn bonding.

The O–Zn average distance is 2.037(5) Å, in accord with average distances in similar binuclear zinc mixed ligand complexes (i.e. [Zn₂(valp)₄(quin)₂] 2.046(0) Å [10], [Zn₂(indo)₄(Py)₂], 2.039(3) Å and [Zn₂(indo)₄(DMA)₂], 2.042(2) Å [32]). The C1–O1, C1–O2 and C14–O3, C14–O4 distances are 1.254(4) Å, 1.250(4) Å and 1.235(4) Å, 1.246(4) Å, respectively, as expected for carboxylates in bridging coordination. The values are close to each other and similar to the corresponding zinc valproate complex (1.253 Å) in bridging coordination mode [10].

The C–O–Zn average angle in **5** is 128.3°, larger than the corresponding metal carboxylates in bridging coordination (i.e. rhodium valproate complexes [118.8°] [33]), which supports the absence of direct Zn⋯Zn bonding.

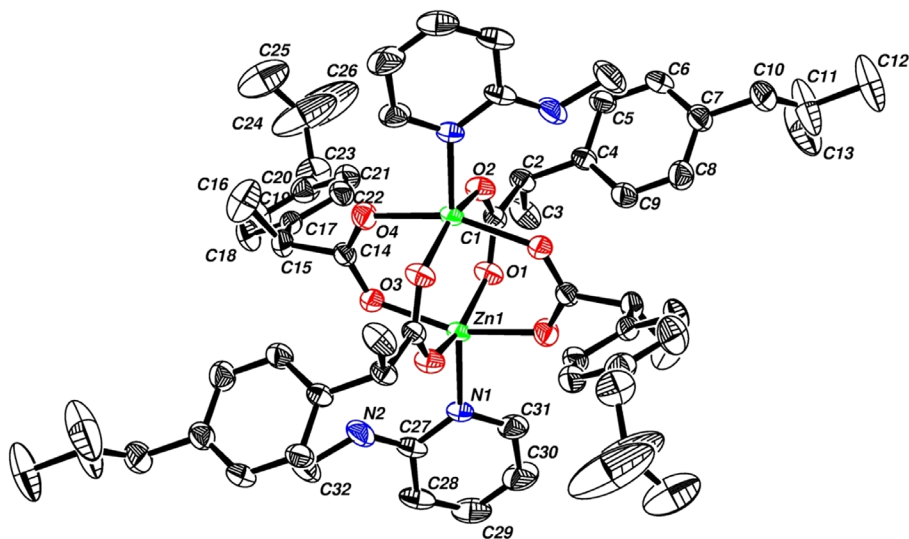


Figure 3. The molecular structure of **5** showing the atom labeling scheme.

Table 2. Selected bond lengths [Å] and angles [°] for **5**.

Bond distance (Å)		Bond angle (°)	
N(1)–Zn(1)	2.030(3)	O(2)#1–Zn(1)–O(3)	87.59(11)
O(2)–Zn(1)#1	2.017(2)	C(14)–O(3)–Zn(1)	132.1(2)
O(4)–Zn(1)#1	2.052(2)	C(14)–O(4)–Zn(1)#1	124.6(2)
Zn(1)–O(2)#1	2.017(2)	O(2)#1–Zn(1)–N(1)	99.91(11)
Zn(1)–O(4)#1	2.052(2)	O(1)–Zn(1)–N(1)	102.44(11)
Zn(1)⋯Zn(1)#1	3.0073(7)	O(2)#1–Zn(1)–Zn(1)#1	75.99(7)

Table 3. Binding modes of **1–5** depending on $^{13}\text{C}\{^1\text{H}\}$ -NMR data.

Compound	$\delta^{13}\text{C}(\text{CH}_3)$ (ppm)	$\delta^{13}\text{C}(\text{CO}_2)$ (ppm)	$\delta^{13}\text{C}(\text{CO}_2)_{\text{cal.}}^*$ (ppm)	Binding mode
H(ibup)	22.47	181.35	158.88	–
Na(ibup)	22.80	201.00	178.20	Ionic
1	22.67	189.46	166.79	Chelating bidentate
2	22.66	179.82	157.16	Monodentate
3	22.68	179.46	156.78	Monodentate
4	22.65	150.01	127.36	Monodentate
5	22.45	181.93	159.48	Bridging bidentate

$$*\delta(\text{CO}_2)_{\text{calculated}} = (\delta^{13}\text{C}(\text{CO}_2) - \delta^{13}\text{C}(\text{CH}_3)).$$

2.4. Infrared and UV-vis spectra

Infrared spectral data of **1–5** from 400 to 4000 cm^{-1} as KBr pellets are summarized in tables S3 and S4. In metal carboxylate complexes, the major characteristics of IR spectra are frequencies of the antisymmetric ($\nu_{\text{as}}(\text{CO}_2)$) and symmetric ($\nu_{\text{s}}(\text{CO}_2)$) stretching vibrations of the carboxylate and the difference between them $\Delta\nu(\text{CO}_2)$. The frequencies of these bands depend upon the coordination mode of the carboxylate. Monodentate binding of the carboxylate group exhibits $\Delta\nu(\text{CO}_2)$ values much higher than the ionic form. Chelating (bidentate) binding of the carboxylate group exhibits $\Delta\nu(\text{CO}_2)$ values significantly lower than the ionic form. The $\Delta\nu(\text{CO}_2)$ values for bridging coordination of the carboxylate are higher than those of chelating mode and close to the ionic values [34], i.e. $\Delta\nu(\text{CO}_2)_{\text{monodentate}} \gg \Delta\nu(\text{CO}_2)_{\text{ionic}} \sim \Delta\nu(\text{CO}_2)_{\text{bridging}} > \Delta\nu(\text{CO}_2)_{\text{chelating}}$. The antisymmetric stretching $\nu_{\text{as}}(\text{CO}_2)$, the symmetric stretching $\nu_{\text{s}}(\text{CO}_2)$ and the difference between these two values of ibuprofen carboxylate in **1–5** and those of sodium ibuprofen are shown in tables S3 and S4.

In **1**, $\nu_{\text{as}}(\text{CO}_2)$ is at 1545 cm^{-1} and $\nu_{\text{s}}(\text{CO}_2)$ at 1414 cm^{-1} , and $\Delta\nu(\text{CO}_2) = 131 \text{ cm}^{-1}$ which is lower than that of sodium ibuprofenate ($\Delta\nu(\text{CO}_2)_{\text{Na(ibup)}} = 150 \text{ cm}^{-1}$) gives an indication that the coordination mode of ibuprofen in **1** is chelating bidentate to form $[\text{Zn}(\text{ibup})_2]$. Dendrinou-Samara *et al.* synthesized $[\text{Zn}(\text{ibup})_2(\text{H}_2\text{O})_2]$ using the same procedure but used methanol/water as solvent; for the complex, $\nu_{\text{as}}(\text{CO}_2)$ occurs at 1605 cm^{-1} and $\nu_{\text{s}}(\text{CO}_2)$ at 1390 cm^{-1} , $\Delta\nu(\text{CO}_2) = 215 \text{ cm}^{-1}$, and they suggest monodentate coordination [16].

Complexes **2** and **3** exhibit $\nu_{\text{as}}(\text{CO}_2)$ at 1624 and 1605 cm^{-1} , $\nu_{\text{s}}(\text{CO}_2)$ occurs at 1352 and 1361 cm^{-1} , respectively, and the $\Delta\nu(\text{CO}_2)$ are 272 and 244 cm^{-1} , respectively, higher than $\Delta\nu(\text{CO}_2)_{\text{Na(ibup)}} = 150 \text{ cm}^{-1}$, which supports monodentate coordination of the ibuprofen carboxylates. This is confirmed by the X-ray structure of **2**. As expected for **2**, two absorption frequencies at 3339 cm^{-1} and 3225 cm^{-1} have been assigned to 1°-NH_2 . The corresponding N–H peak of **2** is lowered by 108 cm^{-1} due to complexation through the pyridine nitrogen. The difference in NH_2 stretching for **2** ($\nu_{\text{as}}(\text{N-H}) - \nu_{\text{s}}(\text{N-H})$) is 114 cm^{-1} , while in free 2-ampy it is 262 cm^{-1} . This indicates a hydrogen-bond in **2** [35], which is confirmed by the crystal structure of **2**.

Complexation of NH_2 will cause a larger shift for the two NH_2 peaks [35]. 2-Aminomethylpy in **3** binds to zinc through pyridine nitrogen and the amino group appears to be in chelating bidentate coordination as supported by the presence of a peak at 3288 cm^{-1} [36–39]. In contrast, two peaks are at 3364 and 3289 cm^{-1} for free 2-aminomethylpy. Metal complexes of 2-aminomethylpy that exhibit strong hydrogen bonding between the amine nitrogens and the carboxylate oxygens show one broad $\nu(\text{NH}_2)$ peak [40]. In addition, **3** shows Zn– NH_2 stretching frequency at 448 cm^{-1} [41].

For **4**, $\nu_{\text{as}}(\text{CO}_2)$ is at 1624 cm^{-1} and $\nu_{\text{s}}(\text{CO}_2)$ is at 1373 cm^{-1} . The high value of $\Delta\nu(\text{CO}_2) = 251 \text{ cm}^{-1}$ is an indication of monodentate coordination of ibuprofen carboxylate since the separation frequency is higher than that of sodium ibuprofen ($\Delta\nu(\text{CO}_2) = 150 \text{ cm}^{-1}$). This value is in agreement with other monodentate zinc carboxylate complexes [42]. Infrared spectra of metal complexes of 2,2'-bipy have been studied extensively [42]. In general, bands at high frequency are not metal-sensitive since they originate from the heterocyclic or aromatic rings of the ligand. Thus, the main interest has focused on the low frequency region, where M–N and other metal sensitive vibrations appear. However, it is difficult

Table 4. *In vitro* antibacterial activity data of **1–4**. Inhibition zone diameter (IZD) in mm, all micro-organisms were resistant to DMSO. The data stated as average \pm standard deviation (N = 3), the concentration was 30 mg 5 mL⁻¹ in DMSO (6 g L⁻¹).

Compound	<i>B. subtilis</i>	<i>M. luteus</i>	<i>S. aureus</i>	<i>E. coli</i>	<i>K. pneumoniae</i>	<i>P. mirabilis</i>
	G+	G+	G+	G–	G–	G–
ZnCl ₂	–	–	–	–	–	–
Na(ibup)	–	–	–	–	–	–
1	10.3 \pm 0.6	11 \pm 1	12 \pm 3	–	–	–
2	–	–	–	–	–	–
3	–	–	–	–	–	–
4	12 \pm 1	13 \pm 3	15 \pm 2	14.1 \pm 0.1	11.3 \pm 0.6	14.1 \pm 0.3
Erythromycin	36.0	37.0	38.0	18.0	21.0	17.0
Gentamycin	25.0	32.0	27.0	28.0	31.0	28.0

“–” indicates zero inhibition.

Table 5. Antibacterial activity data (inhibition zone diameter (IZD) in mm) for **4** and 2,2'-bipy.

Compound	Concentration (g/L DMSO)	<i>B. subtilis</i>	<i>M. luteus</i>	<i>S. aureus</i>	<i>E. coli</i>	<i>K. pneumoniae</i>	<i>P. mirabilis</i>
		G+	G+	G+	G–	G–	G–
4	6	12.3	13.0	15.0	14.1	11.3	14.1
	3	9	8	13	11	8	12
	1.5	–	–	9	8	7	11
2,2'-bipy	6	21	28	12	27	27	22
	3	11	21	10	26	21	19
	1.5	–	15	9	14	15	16

to assign $\nu(\text{M–N})$ empirically since several ligand vibrations also appear in the same frequency region [34]. Peaks at 3127, 3054, 1512 and 761 cm⁻¹ are characteristic of 2,2'-bipy present in **4** [42].

For **5**, $\nu_{\text{as}}(\text{CO}_2)$ is at 1624 cm⁻¹ and $\nu_{\text{s}}(\text{COO}^-)$ is at 1460 cm⁻¹. The value of $\Delta\nu(\text{CO}_2) = 164$ cm⁻¹ is close to the value of sodium ibuprofen ($\Delta\nu(\text{CO}_2) = 150$ cm⁻¹). It is clear from the X-ray crystal structure of **5** (figure 3) that the coordination mode is bridging bidentate as indicated from IR data and $\Delta\nu(\text{CO}_2)$ value.

All the complexes are white, with a d¹⁰ Zn(II). From the results tabulated in table S5, no ligand-to-metal charge-transfer bands are observed. The bands are assigned to intraligand transitions; the spectra of the complexes are similar to those of nitrogen-donor ligands with very small shifts caused by zinc coordination.

2.5. ¹H- and ¹³C{¹H}-NMR

¹H and ¹³C{¹H}-NMR spectral data of ibuprofen and **1–5** are listed in tables S6–S10. Comparison of the ¹H-NMR spectra of **1** and ibuprofen showed the absence of the O–H resonance in addition to slight upfield shift for most resonances. In the ¹³C{¹H}-NMR spectrum of **1**, the C=O resonance was shifted downfield from 181.35 ppm to 189.46 ppm; this deshielding indicates donation of electrons from the ibuprofen carboxylate to Zn(II). Downfield shift for the resonance of carbon adjacent to carbonyl was also observed, i.e. CH 45.08 ppm to 45.32 ppm and CH₃ ppm 18.15 to 19.41 ppm which prove the interaction of the carboxyl part of ibuprofen to Zn(II). For **2–5**, slight shifts in the ¹H- and ¹³C NMR spectra were noticed upon complexation. The integration of the ¹H-NMR signals is used to determine the coordination number of the complexes. The ratio between the nitrogen-based ligands and ibuprofen was 1 : 1 in **2** and **3**, while in **4** and **5**, the ratio was 1 : 2.

The ¹³C{¹H}-NMR chemical shifts of the carboxylate groups depend on the coordination number and the coordination mode of the complexed metal [43]. To determine the carboxylate binding mode, it is necessary to use a reference in the spectra. The terminal methyl group of ibuprofen can be used as a reference which is less affected by complexation. The ¹³C{¹H}-NMR chemical shifts of carbonyl group of different modes are in the following order [43]: $\delta^{13}\text{C}(\text{CO}_2)_{\text{ionic}} > \delta^{13}\text{C}(\text{CO}_2)_{\text{chelating}} > \delta^{13}\text{C}(\text{CO}_2)_{\text{bridging}} > \delta^{13}\text{C}(\text{CO}_2^-)_{\text{monodentate}}$.

Table 6. Minimum inhibition concentrations (MIC, in $\mu\text{g/mL}$) of **4** and 2,2'-bipy.

Compound	<i>B. subtilis</i>	<i>M. luteus</i>	<i>S. aureus</i>	<i>E. coli</i>	<i>K. pneumoniae</i>	<i>P. mirabilis</i>
	G+	G+	G+	G–	G–	G–
4	3000	3000	1500	1500	1500	1500
2,2'-bipy	3000	188	1500	1500	1500	1500

Therefore, the $^{13}\text{C}\{^1\text{H}\}$ -NMR chemical shifts of the carboxylate group were calculated and are tabulated in table 3.

Complexes **2** and **5** show monodentate and bridging bidentate coordination, respectively, and exhibit carboxylate group chemical shift ($\delta(\text{CO}_2)_{\text{cal}}$) values of 157.16 and 159.48 ppm, respectively. In complexes with a $\delta(\text{CO}_2)_{\text{cal}}$ value close to or lower than 157.16 ppm, the carboxylate group was considered as having monodentate coordination. Based on this, in **3** and **4** the ibuprofen carboxylate groups are monodentate which agrees with the results obtained from IR spectroscopy. The crystal structure and $\delta(\text{CO}_2)_{\text{cal}}$ are compatible since, as discussed in the crystal structure of **5**, it is clear that ibuprofen carboxylate groups bind in bidentate bridging coordination. Complex **1** has the highest value of $\delta(\text{CO}_2)_{\text{cal}}$. Therefore, this enforces the results of IR spectroscopy that suggest chelating bidentate mode.

2.6. Antibacterial activity

Before we performed the biological measurements, the solution stability of **1–4** was checked periodically by ^1H - and ^{13}C NMR spectroscopy in chloroform and DMSO solvents. No major changes were observed between the measurements. In addition, the complexes were crystallized by solvent evaporation which took several days and the NMR measurements were repeated to give the same physical properties of the compounds.

Three Gram-positive bacteria (*Micrococcus luteus*, *Staphylococcus aureus* and *Bacillus subtilis*) and three Gram-negative bacteria (*E. coli*, *Klebsiella pneumonia* and *Proteus mirabilis*) were used to test the antibacterial activity of the compounds. The results were obtained by the well-diffusion method using a 30 mg 5 mL^{-1} concentration (in DMSO) with a volume of 50 μL per well. The values of the antibacterial activity are the average of three trials and are stated as average \pm standard error. The results are tabulated in table 4 using DMSO as a negative control while erythromycin and gentamycin were used as positive controls. The sodium ibuprofen and Zn(II) (as ZnCl_2) did not show antibacterial activity against any of the tested microorganisms, and erythromycin and gentamycin as positive controls showed high antibacterial activity against all tested bacterial species with inhibition zone diameter (IZD) of 17–43 and 23–33 mm, respectively.

Complex **1** exhibited antibacterial activity only against Gram-positive bacteria with IZD of 10–12 mm. Complexes **2** and **3** did not exhibit activity against Gram-positive or Gram-negative bacteria. The efficiency of **4** against all tested micro-organisms is good with IZD 11–15 mm. Complex **4** was chosen for further studies because of its higher IZD values. Thus, **4** has been studied with its parent nitrogen-donor ligand 2,2'-bipy against all tested Gram-positive and Gram-negative bacteria; the aim of this step was to determine the effect of the complexation on antibacterial activity. Dilutions of the complex and 2,2'-bipy were prepared in DMSO using the same procedure; the complex and the parent ligand were tested in the same plate to reserve the same conditions for both. All antibacterial results are listed in table 5. It is clear from the results that the complexation of zinc ibuprofen with 2,2'-bipy in **4** has decreased the antibacterial activity against most tested bacteria. The lowest concentration that inhibits bacterial growth is the minimum inhibition concentration (MIC). The MIC values for **4** were compared side by side with those of 2,2'-bipy (table 6). The MIC values for **4** are close to those of free 2,2'-bipy, which indicate a weak effect of complexation on antibacterial activity.

3. Conclusion

The synthesis and characterization of four new Zn(II) complexes with the NSAID ibuprofen in the presence of N-donor heterocyclic ligands 2-ampy, 2-ammethylpy, 2,2'-bipy and 2-methylampy have been achieved. ^1H - and $^{13}\text{C}\{^1\text{H}\}$ -NMR, IR and UV-vis spectroscopies were used to study and characterize the new complexes in addition to X-ray diffraction of **2** and **5**. The results revealed distorted tetrahedral geometry of Zn(II) in **2** with two monodentate ibuprofen ligands and two 2-ampy ligands. The structure of **5** consists of centrosymmetric binuclear Zn units, with four ibuprofen bridging bidentate ligands. Each Zn(II) has a square pyramidal coordination geometry with the apex provided by axial coordination of 2-methylampy. Complexes **3** and **4** are proposed to have monodentate coordination of ibuprofen carboxylate as predicted by NMR, IR and UV-vis results. Complex **4** showed antibacterial activity against G-(+) and G(-) bacteria, whereas the complexation of 2,2'-bipy in **4** decreased the antibacterial activity compared with that of free 2,2'-bipy. Complex **5** did not show any antibacterial activity against G-(+) and G(-) bacteria.

4. Experimental

4.1. Starting materials

Zinc(II) chloride was purchased from Merck, sodium ibuprofen from Sigma and 2-aminopyridine, 2-aminomethylpyridine and 2,2'-bipyridine were purchased from Aldrich. All solvents were of analytical reagent grade and purchased from commercial sources. *M. luteus*, *S. aureus*, *B. subtilis*, *E. coli*, *K. pneumonia*, and *P. mirabilis* were obtained from the Biology and Biochemistry Department at Birzeit University.

4.2. Synthesis

All Zn(II) complexes were synthesized at room temperature in ambient conditions.

4.2.1. Synthesis of the precursor $[\text{Zn}(\text{ibup})_2(\text{H}_2\text{O})_2]$ (**1**)

Ibuprofen (6.18 g, 0.03 mol) was dissolved in a solution of sodium hydroxide (1.20 g, 0.03 mol) in 100 mL water. To this solution, a solution of zinc chloride (2.05 g, 0.015 mol) in 30 mL of water was slowly added with stirring in molar ratio 2 : 1. The mixture was allowed to stir for 1 h, and the precipitate formed was collected, washed with cold water and dried in vacuum.

$[\text{Zn}(\text{ibup})_2(\text{H}_2\text{O})_2]$ (**1**): ~90% (6.50 g) yield, m.p. = 86.8–94.3 °C. ^1H NMR (CDCl_3): δ (ppm) 0.89 (d, 6H, CH_3 , $^3J_{\text{H-H}} = 6.6$ Hz), 1.36 (d, 3H, CH_3 , $^3J_{\text{H-H}} = 6.9$ Hz), 1.82 (m, 1H, CH), 2.42 (d, 2H, CH_2 , $^3J_{\text{H-H}} = 7.2$ Hz), 3.62 (q, 1H, CH, $^3J_{\text{H-H}} = 7.2$ Hz), 7.03 (d, 2H, CH, $^3J_{\text{H-H}} = 8.1$ Hz), 7.15 (d, 2H, CH, $^3J_{\text{H-H}} = 8.1$ Hz). $^{13}\text{C}\{^1\text{H}\}$ -NMR (CDCl_3): δ (ppm) 19.41 (CH_3), 22.67 (CH_3), 30.42 (CH), 45.32 (CH), 47.24 (CH_2), 127.44 (CH), 129.41 (CH), 138.65 (C), 140.51 (C), 189.46 (C=O). IR (cm^{-1} , KBr): 3090 w, 2953 s, 2925 s, 2867 m, 1706 w, 1544 vs 1512 m, 1414 vs 1366 m, 1290 m, 1121 w, 1070 m, 848 m, 786 w, 740 w, 607 w, 548 w, 430 w. UV-vis (EtOH, λ (nm)): 315.

4.2.2. Synthesis of $[\text{Zn}(\text{ibup})_2(2\text{-ampy})_2]$ (**2**)

2-Aminopyridine (0.56 g, 5.95 mmol) was dissolved in acetone and gradually added to stirred acetone solution of **1** (1.43 g, 1.50 mmol). The solution was stirred for 3 h, and then evaporated to dryness under vacuum to get a solid residue. The solid product was washed with ether and allowed to dry in air. Suitable crystals for X-ray structural analysis were obtained by recrystallization from acetone.

$[\text{Zn}(\text{ibup})_2(2\text{-ampy})_2]$ (**2**): ~64% (1.28 g) yield. m.p. = 151.2–152.7 °C. ^1H NMR (CDCl_3): δ (ppm) 0.84 (d, 6H, CH_3 , $^3J_{\text{H-H}} = 6.6$ Hz), 1.32 (d, 3H, CH_3 , $^3J_{\text{H-H}} = 6.9$ Hz), 1.79 (m, 1H, CH_(ibup)), 2.38 (d, 2H, CH_2 , $^3J_{\text{H-H}} = 6.9$ Hz), 3.54 (q, 1H, CH_(ibup), $^3J_{\text{H-H}} = 6.9$ Hz), 6.45 (bs, 2H, NH_2), 6.53 (m, 2H, CH), 7.02 (d, 2H, CH_(ibup), $^3J_{\text{H-H}} = 7.5$ Hz), 7.19 (d, 2H, CH_(ibup), $^3J_{\text{H-H}} = 7.8$ Hz), 7.42 (t, 1H, CH, $^3J_{\text{H-H}} = 9.0$ Hz), 7.74 (d, 1H, CH, $^3J_{\text{H-H}} = 4.8$ Hz). $^{13}\text{C}\{^1\text{H}\}$ -NMR (CDCl_3): δ (ppm) 20.33 (CH_3), 22.66 (CH_3), 30.11 (CH_(ibup)), 44.79 (CH_(ibup)), 46.53 (CH_2), 110.09 (CH), 112.15 (CH), 127.63 (CH_(ibup)), 129.02 (CH_(ibup)), 138.83 (CH), 139.07 (C_(ibup)), 141.23 (C_(ibup)), 147.04 (CH), 160.06 (C-NH₂), 179.82 (C=O). IR (KBr, cm^{-1}): 3370 s, 3339 s, 3225 s, 3030 vw, 2954 s, 2925 m,

2866 m, 1640 s, 1624 vs 1566 s, 1502 vs 1454 s, 1378 s, 1352 s, 1272 s, 1165 m, 1066 m, 1009 m, 885 w, 850 s, 769 s, 740 m, 725 w, 633 w, 543 w, 457 m, 414 w. UV-vis (DMSO, λ (nm)): 301.

4.2.3. Synthesis of [Zn(ibup)₂(2-ammethylpy)] (3)

The same procedure was followed as for **2** except with 2-aminomethylpyridine (0.15 mL, 0.14 g, 1.27 mmol) and **1** (0.30 g, 0.32 mmol).

[Zn(ibup)₂(2-ammethylpy)] (**3**): ~62% (0.27 g) yield. m.p. = 154.8–156.9 °C. ¹H NMR (CDCl₃): δ (ppm) 0.85 (d, 6H, CH₃, ³J_{H-H} = 5.7 Hz), 1.23 (d, 3H, CH₃, ³J_{H-H} = 6.3 Hz), 1.77 (m, 1H, CH_(ibup)), 2.34 (d, 2H, CH_{2(ibup)}, ³J_{H-H} = 6.3 Hz), 3.42 (q, 1H, CH_(ibup), ³J_{H-H} = 7.2 Hz), 3.53 (bs, 2H, NH₂), 3.94 (bd, 2H, CH₂, ³J_{H-H} = 5.4 Hz), 6.96 (d, 2H, CH_(ibup), ³J_{H-H} = 7.5 Hz), 7.10 (d, 2H, CH_(ibup), ³J_{H-H} = 9.6 Hz), 7.35 (t, 1H, CH, ³J_{H-H} = 5.1 Hz), 7.46 (d, 1H, CH, ³J_{H-H} = 7.5 Hz), 7.89 (m, 1H, CH), 8.42 (d, 1H, CH, ³J_{H-H} = 4.8 Hz). ¹³C{¹H}-NMR (CDCl₃): δ (ppm) 20.59 (CH₃), 22.68 (CH₃), 30.13 (CH_(ibup)), 44.76 (CH_(ibup)), 44.88 (CH_{2(ibup)}), 46.99 (CH₂), 122.56 (CH), 123.18 (CH), 127.58 (CH_(ibup)), 128.83 (CH_(ibup)), 136.39 (CH), 138.75 (C_(ibup)), 141.91 (C_(ibup)), 148.11 (CH), 161.07 (C), 179.46 (C=O). IR (KBr, cm⁻¹): 3288 m, 3125 w, 2955 s, 2924 m, 2868 m, 1672 s, 1605 vs 1546 w, 1508 s, 1487 vs 1455 s, 1435 m, 1387 w, 1361 m, 1287 s, 1254 s, 1220 m, 1129 m, 1097s, 1064 s, 1040 m, 1016 m, 877 m, 850 s, 787 m, 759 w, 733 m, 708 s, 673 m, 640 m, 593 m, 491 w, 463 m, 448 s, 441 w. UV-vis (EtOH, λ (nm)): 315. ESI (M⁺-18 = 675.23).

4.2.4. Synthesis of [Zn(ibup)₂(2,2'-bipy)] (4)

The same procedure was followed as for **2** except with 2,2'-bipyridine (0.30 g, 1.92 mmol) and **1** (0.52 g, 0.55 mmol).

[Zn(ibup)₂(2,2'-bipy)] (**4**): ~33% (0.23 g) yield. m.p. = 143.6–146.3 °C. ¹H NMR (CDCl₃): δ (ppm) 0.86 (d, 6H, CH₃, ³J_{H-H} = 6.6 Hz), 1.44 (d, 3H, CH₃, ³J_{H-H} = 6.9 Hz), 1.78 (m, 1H, CH_(ibup), ³J_{H-H} = 6.6 Hz), 2.38 (d, 2H, CH₂, ³J_{H-H} = 7.2 Hz), 3.71 (q, 1H, CH_(ibup), ³J_{H-H} = 7.2 Hz), 6.94 (d, 2H, CH_(ibup), ³J_{H-H} = 9.0 Hz), 7.19 (d, 2H, CH_(ibup), ³J_{H-H} = 9.0 Hz), 7.66 (dd, 1H, CH, ³J_{H-H} = 8.4 Hz), 7.91 (bs, 1H, CH), 8.34 (d, 1H, CH, ³J_{H-H} = 9.0 Hz), 9.02 (d, 1H, CH, ³J_{H-H} = 8.1 Hz). ¹³C{¹H}-NMR (CDCl₃): δ (ppm) 19.82 (CH₃), 22.65 (CH₃), 30.44 (CH_(ibup)), 45.31 (CH_(ibup)), 46.38 (CH₂), 124.76 (CH), 126.68 (CH), 127.30 (CH_(ibup)), 128.57 (CH_(ibup)), 128.79 (CH), 138.43 (C_(ibup)), 139.19 (C_(ibup)), 140.76 (CH), 149.67 (C), 183.41 (C=O). IR (KBr, cm⁻¹): 3127 m, 3054 w, 2961 s, 2864 m, 1624 s, 1512 m, 1456 m, 1373 s, 1275 s, 1159 m, 1001 m, 881 m, 848 m, 800 w, 761 m, 677 m, 593 m, 443 m. UV-vis (EtOH, λ (nm)): 308. ESI (M⁺-18 = 629.11).

4.2.5. Synthesis of [Zn₂(ibup)₄(2-methylampy)₂] (5)

The same procedure was followed as for **2** except with 2-(methylamino)pyridine (0.30 mL, 0.28 g, 2.54 mmol) and **1** (0.60 g, 0.64 mmol).

[Zn₂(ibup)₄(2-methylampy)₂] (**5**): ~75% (0.65 g) yield. m.p. = 135.0–137.0 °C. ¹H NMR (CDCl₃): δ (ppm) 0.91 (d, 6H, CH₃, ³J_{H-H} = 6.3 Hz), 1.39 (d, 3H, CH₃, ³J_{H-H} = 6.9 Hz), 1.84 (m, 1H, CH_(ibup), ³J_{H-H} = 6.6 Hz), 2.43 (d, 3H, CH₃, ³J_{H-H} = 6.9 Hz), 2.53 (s, 3H, NCH₃), 3.54 (q, 1H, CH_(ibup), ³J_{H-H} = 6.9 Hz), 6.37 (d, 2H, CH, ³J_{H-H} = 9.0 Hz), 6.42 (t, 1H, CH, ³J_{H-H} = 6.0 Hz), 7.02 (d, 2H, CH_(ibup), ³J_{H-H} = 7.8 Hz), 7.20 (d, 2H, CH_(ibup), ³J_{H-H} = 7.8 Hz), 7.50 (t, 1H, CH, ³J_{H-H} = 9.0 Hz), 7.72 (d, 1H, CH, ³J_{H-H} = 5.1 Hz). ¹³C{¹H}-NMR (CDCl₃): δ (ppm) 19.77 (CH₃), 22.45 (CH₃), 28.94 (NHCH₃), 30.24 (CH_(ibup)), 45.12 (CH_(ibup)), 47.02 (CH₂), 106.40 (CH), 111.76 (CH), 127.40 (CH_(ibup)), 128.88 (CH_(ibup)), 139.34 (CH), 140.10 (C_(ibup)), 140.35 (C_(ibup)), 146.94 (CH), 159.11 (C–NH), 181.93 (C=O). IR (KBr, cm⁻¹): 3371 s, 3171 vw, 2959 s, 2867 s, 1647 s, 1624 vs 1538 m, 1514 m, 1460 s, 1414 s, 1286 s, 1169 s, 1074 m, 1012 m, 920 m, 888 m, 843 s, 790 m, 761 s, 640 m, 595 s, 496 m, 494 w. UV-vis (DMSO, λ (nm)): 303.

4.3. Physical measurements

Infrared (IR) spectra were recorded from 200 to 4000 cm⁻¹ (KBr) on a Varian 600 FT-IR spectrometer. UV-Vis spectra were recorded using a Hewlett Packard 8453 photodiode array spectrophotometer from 200 to 800 nm using DMSO as solvent. NMR spectra were recorded on a Varian Unity spectrometer

Table 7. Crystal data and structure refinement of **2** and **5**.

	2		5	
Empirical formula	C ₃₆ H ₄₆ N ₄ O ₄ Zn		C ₆₄ H ₈₄ N ₄ O ₈ Zn ₂	
Formula weight	664.14		1168.09	
Temperature	295(1) K		293(1) K	
Wavelength	0.71073 Å		0.71073 Å	
Crystal system	Triclinic		Triclinic	
Space group	P-1		P-1	
Unit cell dimensions	<i>a</i> = 11.166(1) Å	<i>a</i> = 70.797(2)°	<i>a</i> = 10.655(1) Å	<i>a</i> = 97.146(2)°
	<i>b</i> = 11.232(1) Å	<i>β</i> = 81.611(2)°	<i>b</i> = 11.095(1) Å	<i>β</i> = 108.123(2)°
	<i>c</i> = 16.251(2) Å	<i>γ</i> = 75.996(2)°	<i>c</i> = 15.496(2) Å	<i>γ</i> = 108.074(2)°
Volume	1862.6(3) Å ³		1604.9(3) Å ³	
Z	2		1	
Density (calculated)	1.184 Mg m ⁻³		1.209 Mg m ⁻³	
Absorption coefficient	0.699 mm ⁻¹		0.800 mm ⁻¹	
<i>F</i> (0 0 0)	704		620	
Crystal size	0.33 × 0.25 × 0.07 mm ³		0.34 × 0.23 × 0.12 mm ³	
Theta range for data collection	1.88 to 27.99°		2.85 to 27.00°	
Index ranges	−14 ≤ <i>h</i> ≤ 14, −14 ≤ <i>k</i> ≤ 14, −21 ≤ <i>l</i> ≤ 20		−13 ≤ <i>h</i> ≤ 13, −14 ≤ <i>k</i> ≤ 14, −19 ≤ <i>l</i> ≤ 19	
Reflections collected	20,963		17,459	
Independent reflections	8572 [<i>R</i> (int) = 0.0350]		6880 [<i>R</i> (int) = 0.0279]	
Completeness to theta = 27.00°	95.40%		98.0%	
Absorption correction	None		None	
Refinement method	Full-matrix least-squares on <i>F</i> ²		Full-matrix least-squares on <i>F</i> ²	
Data/restraints/parameters	8572/2/409		6880/5/362	
Goodness-of-fit on <i>F</i> ²	0.964		1.069	
Final <i>R</i> indices [<i>I</i> > 2σ(<i>I</i>)]	<i>R</i> 1 = 0.0629, <i>wR</i> 2 = 0.1663		<i>R</i> 1 = 0.0628, <i>wR</i> 2 = 0.1626	
<i>R</i> indices (all data)	<i>R</i> 1 = 0.1191, <i>wR</i> 2 = 0.1978		<i>R</i> 1 = 0.0751, <i>wR</i> 2 = 0.1706	
Largest diff. peak and hole	0.860 and −0.279 e.Å ⁻³		0.776 and −0.364 e.Å ⁻³	

$$^{\circ}R1 = \frac{\sum ||F_o| - |F_c||}{\sum F_o}, wR2 = \frac{\{\sum [w(F_o^2 - F_c^2)^2]\}^{1/2}}{\{\sum [w(F_o^2)^2]\}^{1/2}}$$

operating at 300 MHz for ¹H NMR spectra and 75 MHz for the ¹³C{¹H}-NMR spectra (CDCl₃). Melting points were determined in capillary tubes with EZ-Melt apparatus without any correction.

4.4. X-ray crystallography

X-ray intensity data of **2** and **5** were carried out at room temperature on a Bruker SMART APEX CCD X-ray diffractometer system (graphite-monochromated Mo Kα radiation λ = 0.71073 Å) using SMART software package [44]. The data were reduced and integrated by the SAINT program package [45]. The structure was solved and refined by the SHELXTL software package [46]. Hydrogens were located geometrically and treated with a riding model. Crystal data and details of the data collection and refinement are summarized in table 7.

4.5. Antibacterial activity

Three Gram-positive bacteria (*M. luteus*, *S. aureus*, and *B. subtilis*) and three Gram-negative bacteria (*E. coli*, *K. pneumonia*, and *P. mirabilis*) were used to test antibacterial activity. The tests were carried out using the agar-well diffusion method [47].

The wells (6 mm in diameter) were dug in the media with the help of a sterile glassy borer. Single bacterial colonies were dissolved in sterile saline until the suspended cells reached the turbidity of McFarland 0.5 Standard. The bacterial inocula were spread on the surface of the Muller Hinton nutrient agar with help of a sterile cotton swab. 50 μL of the test samples (30 mg 5 mL⁻¹ DMSO “6 g L⁻¹”) were introduced in the respective wells. Another well was supplemented with DMSO for negative control. The plates were incubated immediately at 37 °C for 24 h. The antibacterial activity was determined by measuring the diameter of complete growth inhibition zone in millimeters (mm). The results are the average of three trials and they are stated as average ± standard deviation.

Complex **4** was selected for further antibacterial studies. Serial dilutions in DMSO of this complex and 2,2'-bipy were prepared. The diluted solutions were tested in similarly prepared DMSO plates using the same procedure. The inhibition zone diameter (IZD) at 30, 15, and 7.5 mg 5 mL⁻¹ DMSO and the minimum inhibition concentration (MIC) were determined for **4** and 2,2'-bipy.

Supplementary material

CCDC 1026551 and CCDC 1432996 contain the supplementary crystallographic data for **2** and **5**. These data can be obtained free of charge via <http://www.ccdc.cam.ac.uk/conts/retrieving.html>, or from the Cambridge Crystallographic Data Center, 12 Union Road, Cambridge CB2 1EZ, UK; Fax: (+44) 1223-336-033; or E-mail: deposit@ccdc.cam.ac.uk. Supplementary data associated with this article can be found in the online version.

Acknowledgement

The authors thank the office of Vice President for Academic Affairs at Birzeit University for their financial support.

Disclosure statement

No potential conflict of interest was reported by the authors.

References

- [1] R.R. Crichton. In *Biological Inorganic Chemistry*, p. 197, Elsevier, Amsterdam (2008).
- [2] L. Cuevas, A. Koyanagi. *Ann. Trop. Paediatrics: Int. Child Health*, **25**, 149 (2005). DOI: [10.1179/146532805X58076](https://doi.org/10.1179/146532805X58076).
- [3] P.M. Harrison, R.J. Hoare. *Metals in Biochemistry*, Chapman and Hall, London (1980).
- [4] J. Osredkar, N. Sustar. *J. Clin. Toxicol.*, **53**, 1 (2011).
- [5] K.Y.S. Keiko, K. Masahiro. *J. Health Sci.*, **52**, 1 (2006).
- [6] V. Zelenák, K. Györyová, D. Mlynarcik. *Met.-Based Drugs*, **8**, 269 (2002).
- [7] S.G.K. Atmaca, R. Çicek. *Turk. J. Med. Sci.*, **28**, 595 (1998).
- [8] E.M.D. Szunyogová, D. Mudroňová, K. Györyová, R. Nemcová, J. Kovářová. *J. Therm. Anal. Calorim.*, **88**, 355 (2007).
- [9] S.-R. Rehman, M. Ikram, S. Rehman, A. Faiz, S. Awaz. *Bull. Chem. Soc. Ethiopia*, **24**, 201 (2010); (a) Marcela Rizzotto (2012). *Metal Complexes as Antimicrobial Agents, A Search for Antibacterial Agents*, Dr. Varaprasad Bobbarala (Ed.), Ch. 5, ISBN: 978-953-51-0724-8, In Tech, Croatia. DOI: <http://dx.doi.org/10.5772/45651>. Available online at: <http://www.intechopen.com/books/a-search-for-antibacterial-agents/metal-complexes-as-antimicrobial-agents>; (b) F. Dimiza, A.N. Papadopoulos, V. Tangoulis, V. Psycharis, C.P. Raptopoulou, D.P. Kessissoglou, G. Psomas. *Dalton Trans.*, **39**, 4517 (2010); (c) F. Dimiza, S. Fountoulaki, A.N. Papadopoulos, C.A. Kontogiorgis, V. Tangoulis, C.P. Raptopoulou, V. Psycharis, A. Terzis, D.P. Kessissoglou, G. Psomas. *Dalton Trans.*, **40**, 8555 (2011); (d) S. Fountoulaki, F. Perdih, I. Turel, D.P. Kessissoglou, G. Psomas. *J. Inorg. Biochem.*, **105**, 1645 (2011); (e) C. Tolia, A.N. Papadopoulos, C.P. Raptopoulou, V. Psycharis, C. Garino, L. Salassa, G. Psomas. *J. Inorg. Biochem.*, **123**, 53 (2013); (f) F. Dimiza, A.N. Papadopoulos, V. Tangoulis, V. Psycharis, C.P. Raptopoulou, D.P. Kessissoglou, G. Psomas. *J. Inorg. Biochem.*, **107**, 54 (2012); (g) S. Tsiliou, L.-A. Kefala, F. Perdih, I. Turel, D.P. Kessissoglou, G. Psomas. *Eur. J. Med. Chem.*, **48**, 132 (2012); (h) M. Zampakou, N. Rizeq, V. Tangoulis, A.N. Papadopoulos, F. Perdih, I. Turel, G. Psomas. *Inorg. Chem.*, **53**, 2040 (2014).
- [10] M. Darawsheh, H. Abu Ali, A.L. Abuhijleh, E. Rappocciolo, M. Akkawi, S. Jaber, S. Maloul, Y. Hussein. *Eur. J. Med. Chem.*, **82**, 152 (2014).
- [11] (a) H. Abu Ali, M.D. Darawsheh, E. Rappocciolo. *Polyhedron*, **61**, 235 (2013); (b) H. Abu Ali, B. Jabali. *Polyhedron*, **107**, 235 (2016).
- [12] H. Abu Ali, H. Fares, M. Darawsheh, E. Rappocciolo, M. Akkawi, S. Jaber. *Eur. J. Med. Chem.*, **89**, 67 (2015).
- [13] E. Szunyogová, K. Györyová, D. Hudcová, L. Píknová, J. Chomič, Z. Vargová, V. Zelenák. *J. Therm. Anal. Calorim.*, **88**, 219 (2007).
- [14] P.M. Fraser, R. Doll, M.J.S. Langman, J.J. Misiewicz, H.H. Shawdon. *Gut*, **13**, 459 (1972).
- [15] P. Simkin. *The Lancet*, **308**, 539 (1976).
- [16] C. Dendrinou-Samara, G. Tsotsou, L.V. Ekateriniadou, A.H. Kortsaris, C.P. Raptopoulou, A. Terzis, D.A. Kyriakidis, D.P. Kessissoglou. *J. Inorg. Biochem.*, **71**, 171 (1998).
- [17] A.K. Singla, D.K. Mediratta, K. Pathak. *Int. J. Pharm.*, **60**, 27 (1990).
- [18] A.K. Singla, H. Wadhwa. *Int. J. Pharm.*, **108**, 173 (1994).
- [19] A.K. Singla, H. Wadhwa. *Int. J. Pharm.*, **120**, 145 (1995).
- [20] D. Kovala-Demertzi, A. Theodorou, M.A. Demertzi, C.P. Raptopoulou, A. Terzis. *J. Inorg. Biochem.*, **65**, 151 (1997).
- [21] A.L. Abuhijleh. *J. Inorg. Biochem.*, **55**, 255 (1994).

- [22] A.E. Underhill, S.A. Bougourd, M.L. Flugge, S.E. Gale, P.S. Gomm. *J. Inorg. Biochem.*, **52**, 139 (1993).
- [23] J.E. Weder, T.W. Hambley, B.J. Kennedy, P.A. Lay, D. MacLachlan, R. Bramley, C.D. Delfs, K.S. Murray, B. Moubaraki, B. Warwick, J.R. Biffin, H.L. Regtop. *Inorg. Chem.*, **38**, 1736 (1999).
- [24] C. Dendrinou-Samara, P.D. Jannakoudakis, D.P. Kessissoglou, G.E. Manoussakis, D. Mentzafos, A. Terzis. *J. Chem. Soc., Dalton Trans.*, 3259, (1992).
- [25] C. Dendrinou-Samara, D.P. Kessissoglou, G.E. Manoussakis, D. Mentzafos, A. Terzis. *J. Chem. Soc., Dalton Trans.*, 959, (1990).
- [26] A.L. Abuhijleh. *Polyhedron*, **16**, 733 (1997).
- [27] M.E. Katsarou, E.K. Efthimiadou, G. Psomas, A. Karaliota, D. Vourloumis. *J. Med. Chem.*, **51**, 470 (2008).
- [28] S. Shanmuga Sundara Raj, H.-K. Fun, P.-S. Zhao, F.-F. Jian, L.-D. Lu, X.-J. Yang, X. Wang. *Acta Crystallogr.*, **56**, 742 (2000).
- [29] J.Z. Wang, L. Cheng. *Acta Crystallogr., Sect. C*, **65**, m950 (2009).
- [30] M. Harvey, S. Baggio, R. Baggio, A.W. Momburú. *Acta Crystallogr., Sect. C*, **55**, 308 (1999).
- [31] S. Vagin, A.K. Ott, B. Rieger. *Chem. Ing. Tech.*, **79**, 767 (2007).
- [32] Q. Zhou, T.W. Hambley, B.J. Kennedy, P.A. Lay. *Inorg. Chem.*, **42**, 8557 (2003).
- [33] A.L. Abuhijleh, H. Abu Ali, A.H. Emwas. *J. Organomet. Chem.*, **694**, 3590 (2009).
- [34] K. Nakamoto. *Infrared and Raman Spectra of Inorganic and Coordination Compounds*, 6th Edn, Wiley, Hoboken, NJ (2009).
- [35] S. Dinkov, M. Arnaudov. *Spectrosc. Lett.*, **32**, 165 (1999).
- [36] M. Barquín, M.J. González Garmendia, L. Larrinaga, E. Pinilla, M.R. Torres. *Inorg. Chim. Acta*, **362**, 2334 (2009).
- [37] S. Bruda, M.M. Turnbull, C.P. Landee, Q. Xu. *Inorg. Chim. Acta*, **359**, 298 (2006).
- [38] S.S. Tandon, S. Chander, L.K. Thompson. *Inorg. Chim. Acta*, **300–302**, 683 (2000).
- [39] S. Tanase, M. Ferbinteanu, M. Andruh, C. Mathonière, I. Strenger, G. Rombaut. *Polyhedron*, **19**, 1967 (2000).
- [40] V.T. Yilmaz, S. Caglar, W.T.A. Harrison. *Z. Anorg. Allg. Chem.*, **630**, 1512 (2004).
- [41] M.L. Niven, G.C. Percy, D.A. Thornton. *J. Mol. Struct.*, **68**, 73 (1980).
- [42] S. Sen, S. Mitra, P. Kundu, M.K. Saha, C. Krüger, J. Bruckmann. *Polyhedron*, **16**, 2475 (1997).
- [43] C.H. Goh, P.W.S. Heng, E.P.E. Huang, B.K.H. Li, L.W. Chan. *J. Antimicrob. Chemother.*, **62**, 105 (2008).
- [44] SMART-NT V5.6, Bruker AXS GMBH, D-76181 Karlsruhe, Germany (2002).
- [45] SAINT-NT V5.0, BRUKER AXS GMBH, D-76181 Karlsruhe, Germany (2002).
- [46] SHELXTL-NT V6.1, BRUKER AXS GMBH, D-76181 Karlsruhe, Germany (2002).
- [47] M.I. Atta-ur-Rahman, W.J. Choudhary. *Bioassay Techniques for Drug Development.*, Harwood Academic, Amsterdam (2001).